Surface Chemistry in a Zeolite Matrix. Well-Defined Dinitrogen Complexes of Rhodium Supported on Dealuminated Y Zeolite

Hans Miessner*

Contribution from the Zentrum für Heterogene Katalyse, KAIe.V., Rudower Chaussee 5, 12484 Berlin, Germary

Received May 20, 1994[⊗]

Abstract: Surface reactions of well-defined Rh dicarbonyl $Rh^{I}(CO)_2^+$ supported on highly dealuminated Y zeolites (Si:Al ≥ 100) have been monitored by time-resolved FTIR spectroscopy. $Rh^{I}(CO)_2^+$ is partly decarbonylated in an atmosphere of diluted hydrogen at 200-250 °C, yielding a reactive monocarbonyl with $\nu(CO) = 2096$ cm^{-1}. In a gas flow of pure nitrogen this monocarbonyl transforms in dinitrogen complexes of Rh attached to the zeolite framework. Two well-defined dinitrogen complexes of Rh have been identified on the surface: a bis-dinitrogen complex $Rh^{I}(N_2)_2^+$ with $\nu(N_2) = 2244$ and 2218 cm^{-1} and a mixed carbonyl-dinitrogen complex $Rh^{I}(CO)(N_2)^+$ with $\nu(N_2) = 2252$ and $\nu(CO) = 2062$ cm^{-1}. The composition of these surface species has been verified by ligand exchange with $^{15}N_2$ and $C^{18}O$ and a corresponding force field calculation. The force constants of the CO and the N_2 stretchings are lower and higher, respectively, in the mixed carbonyl-dinitrogen complex $Rh^{I}(CO)(N_2)^+$ compared with those of the dicarbonyl and the bis-dinitrogen species, reflecting the weaker π-acceptor ability of N_2 compared with CO. The new complexes are stable in flowing pure nitrogen at temperatures up to 250 °C. They react with CO, yielding the dicarbonyl, and with H_2/N_2, forming reversibly the intermediate monocarbonyl.

Introduction

Transition metal complexes with molecular dinitrogen as ligand(s) have been studied extensively in the past. These studies have been mainly stimulated by the comparison of dinitrogen as a ligand with the isoelectronic carbonyl ligand and by the potential of such complexes as models for nitrogen fixation.[1] While the number of molecular structures containing molecular nitrogen is continuously increasing, attempts to attach such complexes or to synthesize them on the surface of inorganic materials have generally not been successfully.

The interaction of molecular nitrogen with supported transition metals is, on the other hand, rather weak and could be observed normally only at high pressures and/or at low temperatures. In contrast to the adsorption of CO on supported metals, the number of papers devoted to the adsorption of molecular nitrogen is, therefore, limited.[2] Molecular nitrogen was found to adsorb linearly on the metal surface with IR stretching bands usually higher 2200 cm^{-1}.

For supported Rh, an interaction with dinitrogen has been observed also at higher temperatures. In these cases, Rh was supported on TiO_2[3,4] or promoted with alkali[5] and the interaction of N_2 was supposed to take place rather with the partially reduced TiO_2[4] or with the alkali promoter.[2j] Similarly, an IR band at 2063 cm^{-1}, which was detected after the interaction of molecular nitrogen with Rh supported on NaY zeolite at temperatures higher than 200 °C, was suggested to be the result of a reaction with the sodium cations in the zeolite.[6]

An interaction of N_2 with Rh supported on SiO_2[7] or on Al_2O_3[8,9] has been found at low temperatures[7,8] or at high pressures[9] using IR spectroscopy. Besides N_2 species linearly adsorbed on metallic Rh with dinitrogen stretching $\nu(N_2) = 2256-2257$ cm^{-1}, in these works also the existence of nitrogen species on cationic $Rh^{\delta+}$ sites with $\nu(N_2) = 2301-2303$ and 2270-2276 cm^{-1} has been postulated.[8,9]

Highly dealuminated Y zeolite (US-Ex, DAY) has been found to be a unique material to stabilize well-defined cationic surface complexes of transition metals.[10-13] These complexes are probably localized at cationic positions in the supercage near

* Present address: ENIRICERCHE S.p.A., CATA, Via Maritano, 26, I-20097 San Donato Milanese, Italy.

⊗ Abstract published in *Advance ACS Abstracts*, November 1, 1994.

(1) See, for example: (a) Sellmann, D. *Angew. Chem.* **1974**, *86*, 692-702. (b) Chatt, J.; Dilworth, J. R.; Richards, R. L. *Chem. Rev.* **1978**, *78*, 589-625. (c) Henderson, R. A.; Leigh, G. J.; Pickett, C. J. *Adv. Inorg. Chem. Radiochem.* **1983**, *27*, 197-293. (d) Leigh, G. J. *Acc. Chem. Res.* **1992**, *25*, 177-181. (e) Shilov, A. E. *New J. Chem.* **1992**, *16*, 213-218. (f) Shilov, A. E. *Pure Appl. Chem.* **1992**, *64*, 1409-1420.

(2) (a) Eischens, R. P.; Jacknow, J. In *Proceedings of the Third International Congress on Catalysis*; Sachtler, W. M. H., Schuit, G. C. A., Zwietering, P., Eds.; North-Holland Publishing Co.: Amsterdam, 1965; pp 627-643. (b) Nakata, T.; Matsushita, S. *J. Catal.* **1965**, *4*, 631-632. (c) VanHardeveld, R.; VanMontfoort, A. *Surf. Sci.* **1966**, *4*, 396-430. (d) Chernikov, S. S.; Kuz'min, S. G.; Borod'ko, Y. G. *Russ. J. Phys. Chem.* **1968**, *42*, 2038-2040. (e) Mertens, F. P.; Eischens, R. P. In *Structure and Chemistry of Solid Surfaces*; Somorjai, G. A., Ed.; J. Wiley: New York, 1969; Paper 53. (f) Egerton, T. A.; Sheppard, N. *J. Chem. Soc., Faraday Trans.* **1974**, *70*, 1357-1365. (g) Okawa, T.; Onishi, T.; Tamaru, K. *Z. Phys. Chem.* (N.F.) **1977**, *107*, 239-243. (h) Kinoshita, N.; Kido, K.; Domen, K.; Aika, K.; Onishi, T. *J. Chem. Soc., Faraday Trans. 1* **1986**, *82*, 2269-2276. (i) Ravi, A.; King, D. A.; Sheppard, N. *Trans Faraday Soc.* **1986**, *64*, 3358. (j) Kubota, J.; Aika, K. *J. Chem. Soc., Chem. Commun.* **1991**, 1544-1545.

(3) Resasco, D.; Haller, G. L. *J. Chem. Soc., Chem. Commun.* **1980**, 1150-1151.

(4) Vishwanathan, V. *J. Chem. Soc., Chem. Commun.* **1989**, 848-849.

(5) Oh-kita, M.; Aika, K.; Urabe, K.; Ozaki, A. *J. Chem. Soc., Chem. Commun.* **1975**, 147-148.

(6) Basini, L.; Patrini, R.; Aragno, A.; Gates, B. C. *J. Mol. Catal.* **1991**, *70*, 29-42.

(7) Borod'ko, Y. G.; Lyutov, V. S. *Kinet. Katal.* **1971**, *92*, 238.

(8) Wang, H. P.; Yates, J. T., Jr. *J. Phys. Chem.* **1984**, *88*, 852-856.

(9) (a) Wey, J. P.; Burkett, H. D.; Neely, W. C.; Worley, S. D. *J. Am. Chem. Soc.* **1991**, *113*, 2919-2922. (b) Wey, J. P.; Neely, W. C.; Worley, S. D. *J. Phys. Chem.* **1991**, *95*, 8879-8881.

(10) (a) Burkhard, I.; Gutschick, D.; Lohse, U.; Miessner, H. *J. Chem. Soc., Chem. Commun.* **1987**, 291-292. (b) Miessner, H.; Burkhardt, I.; Gutschick, D.; Zecchina, A.; Morterra, C.; Spoto, G. *J. Chem. Soc., Faraday Trans. 1* **1989**, *85*, 2113-2126.

(11) Landmesser, H.; Miessner, H. *J. Phys. Chem.* **1991**, *95*, 10544-10546.

0002-7863/94/1516-11522$04.50/0

the remaining Al atoms in the zeolite framework. Due to the high Si:Al ratio, the complexes are isolated from each other like in a matrix and there are no water or other cations in the zeolite micropores to interact with. These properties result in unusually sharp ($\nu_{1/2} \leq 5$ cm^{-1}) infrared bands of the attached complexes, which allows a detailed structural characterization, e.g. by the identification of the ^{13}CO satellites and of combination bands in the spectra or by a ligand exchange with isotopically labeled ligands combined with a corresponding force field calculation. Thus, we could characterize the surface structures of subcarbonyls of Rh,[10] Ru,[11] and Ir[12] and of nitrosyls and mixed carbonyl nitrosyls of Rh.[13] As we will show in the present work, these well-defined surface species can also be used as the starting material to a surface chemistry, to the formation of other well-defined surface complexes.[14]

Experimental Section

Two differently dealuminated Y zeolites with similar chemical compositions but with different mesopore structures have been used as supports: (i) Y zeolite dealuminated by exchange of the Al atoms in the framework by treating the NaY with $SiCl_4$ (DAY, kindly supplied by DEGUSSA, Germany) having a Si:Al ratio $\geq$ 100 and a mesopore volume of ca. 0.02 cm^3/g and (ii) Y zeolite dealuminated by a hydrothermal treatment of NH_4Y and a subsequent extraction of the nonframework alumina species by leaching with diluted hydrochloric acid (US-Ex, kindly supplied by Dr. U. Lohse, Berlin) having a Si:Al ratio $\sim$ 100 and a mesopore volume of ca. 0.2 cm^3/g. The supports were used in the H form as supplied.

Rh/DAY and Rh/US-Ex (1 wt % Rh) were prepared by impregnating the supports with an appropriate amount of $RhCl_3$ in ethanolic solution and drying the sample at 120 °C in air. The transmission IR studies were performed with self-supported wafers using a special infrared cell made from stainless steel for in-situ measurements up to 400 °C and 50 bar, connected to a gas flowing system, which allows a fast variation of the feed gas. The experiments of the present work were performed at atmospheric pressure. Part of the experiments (using $C^{18}O$) were performed in a conventional glass cell connected with the gas flowing system and with a vacuum line to allow in-situ pretreatment and dosing of probe molecules. As pretreatment, the samples were treated in the IR cell in a flow of pure oxygen (10 mL/min) at 400 °C for at least 2 h. The gas flow through the IR cell was controlled by using electronic flow controllers. The gases used were of high purity: H_2, 99.999%; N_2, 99.996%; 5% CO/Ar (AGA Edelgas GmbH, Berlin); Argon, 99.998% (TEGA, Berlin); $^{15}N_2$, 99.7 atom % $^{15}N_2$ (ISOTEC, Paris). They were additionally purified using OXYSORB units (Messer Griesheim).

The spectra were recorded with a BIORAD FTS 60A spectrometer, normally at a resolution of 2 cm^{-1} coadding 256 scans to obtain a sufficient signal-to-noise ratio. For time-resolved measurements, 64 scans were coadded at a resolution of 4 cm^{-1}. The spectra shown in this paper are corrected for the background and for the contribution of the windows. For the quantitative evaluation, SPECTRACALC and STATGRAPHICS were used.

Results and Discussion

Formation of Rh Dicarbonyl. As the first step, the well-defined Rh dicarbonyl was produced in the cavities of the zeolite as the starting material for the subsequent surface chemistry. The calcined samples of Rh supported on DAY or US-Ex were treated, therefore, in a stream of 5% CO in Argon at 150 °C.

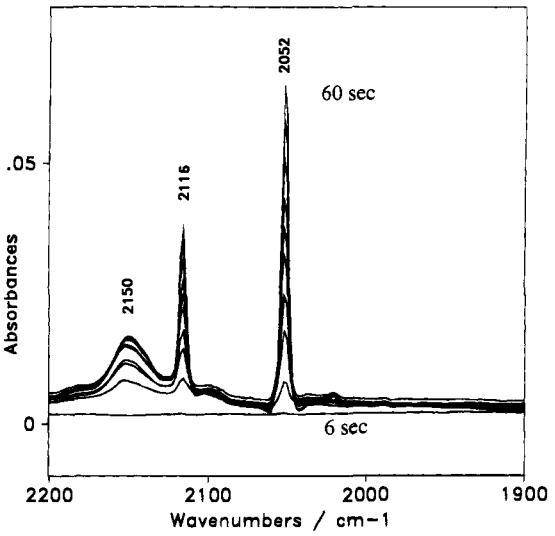

Figure 1. Infrared spectra in the carbonyl stretching region obtained during the first 1 min of the interaction of 5% CO/Ar with Rh/DAY at 150 °C. The increasing carbonyl bands are shown at a time resolution of 6 s. The spectrum in flowing nitrogen at 150 °C before introducing CO/Ar is used as a reference.

Figure 1 shows the evaluation of sharp IR bands at 2116 and 2052 cm^{-1} during the first 1 min of the interaction with CO, taken at a time resolution of 6 s. Besides these bands, a small sharp band at 2019 cm^{-1} and a broader one centered at ca. 2150 cm^{-1} are growing up.

The redox chemistry of highly dispersed Rh supported on inorganic materials during calcination and interaction with CO has been studied previously.[15] With the highly dealuminated Y zeolites as the support, Rh has been found mainly as dispersed Rh_2O_3 after calcination at 400 °C.[16] The interaction with CO at 150 °C results in a reduction of Rh^{3+} to Rh^+ and in the formation of Rh dicarbonyl species on the surface.[10,15,16] The bands at 2116 and 2052 cm^{-1} are assigned to a well-defined Rh dicarbonyl with C_{2v} symmetry, $Rh^I(CO)_2^+$, with carbonyl stretching bands at 2118 and 2053 cm^{-1} at room temperature.[10] The band at 2019 cm^{-1} is the ^{13}CO satellite of this surface species due to the natural abundance of 1.1% ^{13}CO in the carbon monoxide.[10] The broader band at 2150 cm^{-1} should be assigned

(12) Burkhardt, I.; Gutschick, D.; Landmesser, H.; Miessner, H. In *Zeolite Chemistry and Catalysis*, Proceedings of the International Symposium, Prague, September 8–13, 1991; Jacobs, P. A., Jaeger, N. I., Kubelkova, I., Wichterlova, B., Eds.; *Stud. Surf. Sci. Catal.* **1991**, *69*, 215–222.

(13) (a) Miessner, H.; Burkhardt, I.; Gutschick, D.; Zecchina, A.; Morterra, C.; Spoto, G. *J. Chem. Soc., Faraday Trans.* **1990**, *86*, 2321–2327. (b) Miessner, H.; Burkhardt, I.; Gutschick, D. *J. Chem. Soc., Faraday Trans.* **1990**, *86*, 2329–2335.

(14) Some of the results presented here were the subject of a preliminary communication: Miessner, H. *J. Chem. Soc., Chem. Commun.* **1994**, 927–928.

(15) (a) Yang, A. C.; Garland, C. W. *J. Phys. Chem.* **1957**, *61*, 1504–1512. (b) Primet, M.; Vedrine, J. C.; Naccache, C. *J. Mol. Catal.* **1978**, *4*, 411–421. (c) Rice, C. A.; Worley, S. D.; Curtis, C. W.; Guin, J. A.; Tarrer, A. R. *J. Chem. Phys.* **1981**, *74*, 6487–6497. (d) Shannon, R. D.; Vedrine, J. C.; Naccache, C.; Lefebvre, F. *J. Catal.* **1984**, *88*, 431–447. (e) Rode, E. J.; Davis, M. E.; Hanson, B. E. *J. Catal.* **1985**, *96*, 574–585. (f) van't Blick, H. F. J.; van Zon, J. B. A. D.; Huizinga, T.; Vis, J. C.; Koningsberger, D. C.; Prins, R. *J. Am. Chem. Soc.* **1985**, *107*, 3139–3147. (g) Miessner, H.; Gutschick, D.; Ewald, H.; Müller, H. *J. Mol. Catal.* **1986**, *36*, 359–373. (h) Bergeret, G.; Gallezot, P.; Gelin, P.; Ben Taarit, Y.; Lefebvre, F.; Naccache, C.; Shannon, R. D. *J. Catal.* **1987**, *104*, 279–287. (i) Zaki, M. I.; Kunzmann, G.; Gates, B. C.; Knözinger, H. *J. Phys. Chem.* **1987**, *91*, 1486–1493. (j) Takahashi, N.; Mijin, A.; Ishikawa, T.; Nobuka, K.; Suematsu, H. *J. Chem. Soc., Faraday Trans. 1* **1987**, *83*, 2605–2617. (k) Keyes, M. P.; Watters, K. L. *J. Catal.* **1988**, *110*, 96–102. (l) Basu, P.; Panayotov, D.; Yates, J. T., Jr. *J. Am. Chem. Soc.* **1988**, *110*, 2074–2081. (m) Wong, C.; McCabe, R. W. *J. Catal.* **1989**, *119*, 47–64. (n) Dictor, R.; Roberts, S. *J. Phys. Chem.* **1989**, *93*, 2526–2532. (o) Solymosi, F.; Knözinger, H. *J. Chem. Soc., Faraday Trans.* **1990**, *86*, 389–395. (p) Buchanan, D. A.; Hernandez, M. E.; Solymosi, F.; White, J. M. *J. Catal.* **1990**, *125*, 456–466. (q) Rao, L.-F.; Fukuoka, A.; Kosugi, N.; Kuroda, H.; Ichikawa, M. *J. Phys. Chem.* **1990**, *94*, 5317–5327. (r) Blackmond, D. G.; Swid, K. P.; Davis, M. E.; Gallezot, P. *J. Catal.* **1990**, *122*, 247–255. (s) Mcquire, M. W.; Mcquire, G. W.; Rochester, C. H. *J. Chem. Soc., Faraday Trans.* **1992**, *88*, 1203–1209. (t) Basini, L.; Marchionna, M.; Aragno, A. *J. Phys. Chem.* **1992**, *96*, 9431–9441. (u) Wong, T. T. T.; Stakheev, A. Y.; Sachtler, W. M. H. *J. Phys. Chem.* **1992**, *96*, 7733–7740. (v) Solymosi, F.; Bansagi, T. *J. Phys. Chem.* **1993**, *97*, 10133–10138.

(16) Schlegel, L.; Miessner, H.; Gutschick, D. *Catal. Lett.* **1994**, *23*, 215–226.

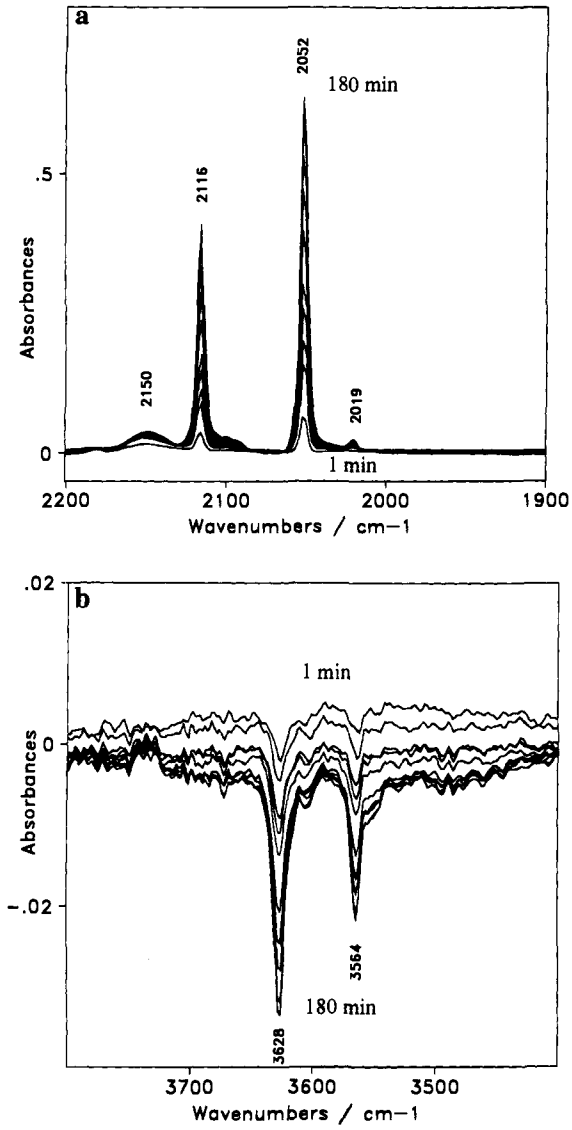

Figure 2. Infrared spectra in the carbonyl stretching region (a) and the hydroxyl stretching region (b) obtained during the interaction of 5% CO/Ar with Rh/DAY at 150 °C after 1, 5, 10, 20, 30, 60, 90, 120, 150, and 180 min, respectively. The spectrum in flowing nitrogen at 150 °C before introducing CO/Ar is used as a reference.

to CO adsorbed nonspecifically on Rh sites in a higher oxidation state, most probably on Rh^{3+}. Stretching frequencies of CO bonded to Rh^{3+} have been reported to fall in the region of 2125–2178 cm^{-1}.[10,15b-d,17]

With increasing time on the stream, the bands of the dicarbonyl grow up to a saturation value as shown in Figure 2a. Simultaneously, the intensity of bands in the OH stretching region of the zeolite at 3628 and 3664 cm^{-1} decreases as shown in the difference spectra in Figure 2b. These bands are assigned to the acid framework hydroxyl groups in the zeolite bridging the remaining Al atoms in the dealuminated framework with the Si atoms.[18] The loss of intensity of these bands during the formation of the dicarbonyl indicates an ion exchange process, exchanging the protons of the acid sites for the $Rh^{I}(CO)_2^+$ cations.[16] The surface reaction could be described schematically by the overall equation:

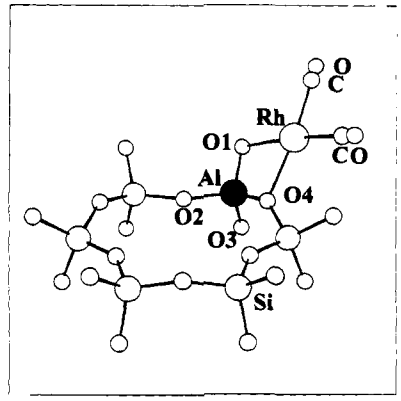

Figure 3. Molecular structure of the $Rh^{I}(CO)_2^+$ complex attached to the zeolite framework, drawn with MOLDRAW.[19] The framework oxygen atoms are numbered according to ref 20.

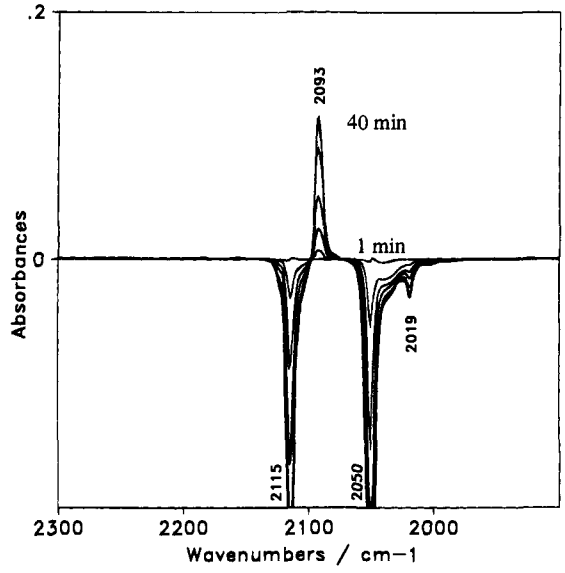

Figure 4. Infrared difference spectra in the carbonyl stretching region obtained during the interaction of Rh dicarbonyl on Rh/DAY with 10% H_2/N_2 at 250 °C after 1, 2, 5, 10, 20, 30, and 40 min, respectively. The spectrum of Rh/DAY after the formation of Rh dicarbonyl in CO/Ar as in Figure 2 and a subsequent flushing with nitrogen at 250 °C is used as a reference.

$$Rh_2O_3 + 6CO + 2O_zH \rightarrow 2O_zRh^{I}(CO)_2 + 2CO_2 + H_2O$$

where O_z designates a zeolite framework oxygen of a structural acid site. Like in molecular analogues, we would expect for the surface species a planar coordination to two zeolite framework oxygens to complete the coordination sphere of the d^8 Rh^+ cation. A possible molecular structure is shown in Figure 3, where the complex is assumed to be located in the supercage and attached to the framework oxygen atoms near to one of the remaining Al atoms. The Rh dicarbonyl complexes are stable in flowing nitrogen or in vacuum up to 250 °C but undergo a reaction with hydrogen as will be shown in the next section.

Formation of the Intermediate Monocarbonyl. The difference spectra in Figure 4 show the results of the transformation of the surface dicarbonyl during a treatment of the sample in a flow of hydrogen in nitrogen (1:10) at 250 °C. The intensity of the carbonyl stretching bands at 2115 and 2050 cm^{-1}

(17) Mattera, V. D., Jr.; Squattriro, P. J.; Risen, W. M., Jr. *Inorg. Chem.* **1984**, *23*, 3597–3601.

(18) (a) Jacobs, P. A.; Uytterhoeven, J. B. *J. Chem. Soc., Faraday Trans. 1* **1973**, *69*, 359–372. (b) Jacobs, P. A.; Uytterhoeven, J. B. *J. Chem. Soc., Faraday Trans. 1* **1973**, *69*, 373–386.

(19) Ugliengo, P.; Borzani, G.; Viterbo, D. *J. Appl. Crystallogr.* **1988**, *21*, 75.

(20) Olson, D. H.; Dempsey, E. *J. Catal.* **1969**, *13*, 221–231.

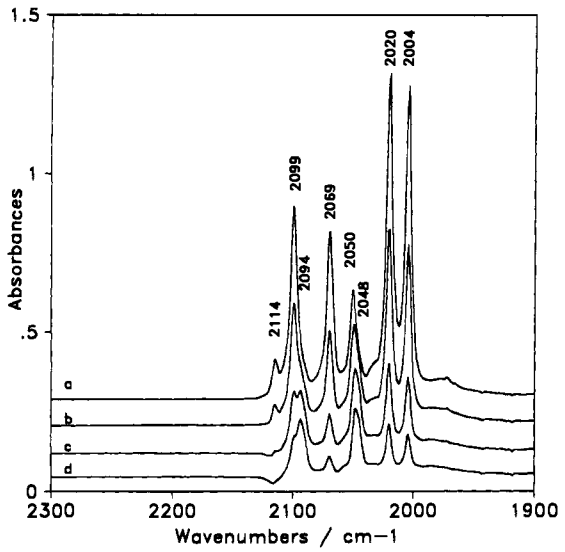

Figure 5. Infrared spectra in the carbonyl stretching region of Rh/US-Ex during the interaction of Rh dicarbonyl with 50% H_2/N_2 at 250 °C after 5 (a), 15 (b), 30 (c), and 40 (d) min. Rh dicarbonyl was previously prepared using a mixture of $C^{16}O:C^{18}O \sim 1:2$.

decreases together with that of the ^{13}CO satellite at 2019 cm^{-1}, and simultaneously, a new carbonyl stretching band at 2093 cm^{-1} appears. There are no other bands appearing in the spectrum, in particular in the region of bridging CO ligands at 1760 or 1830 cm^{-1}, which could be assigned together with the band at 2093 cm^{-1} to a metallic polynuclear Rh cluster such as $Rh_6(CO)_{16}$.[15e,h,q,u] The band at 2093 cm^{-1} was consequently assigned to a monocarbonyl. The same species is formed if argon is used instead of nitrogen to dilute the hydrogen. Also, an exchange of H_2 for D_2 does not change the spectrum of the surface species. With pure hydrogen, a rapid and complete decarbonylation occurs at temperatures higher 200 °C.

Once formed, the monocarbonyl is stable at temperatures ≤200 °C in diluted hydrogen and in vacuum. It is, on the other hand, highly reactive toward traces of CO, yielding again the dicarbonyl.

To prove the structure of the monocarbonyl as proposed, the formation of this species has been performed by starting with a dicarbonyl partially exchanged with $C^{18}O$. Figure 5 shows the IR spectra taken during the interaction with diluted hydrogen at 250 °C. The spectrum of the dicarbonyl species at the starting point (Figure 5, spectrum a) shows carbonyl stretching bands at 2114 + 2050 cm^{-1}, 2099 + 2020 cm^{-1}, and 2069 + 2004 cm^{-1}, that corresponds to the spectra obtained for a partially exchanged dicarbonyl at room temperature with 2118 + 2053 cm^{-1} for $Rh^I(C^{16}O)_2^+$, 2102 + 2022 cm^{-1} for $Rh^I(C^{16}O)(C^{18}O)^+$, and 2072 + 2007 cm^{-1} for $Rh^I(C^{18}O)_2^+$.[10]

During the treatment in the H_2/N_2 flow at 250 °C, the intensities of bands due to the dicarbonyl species are considerably decreased and new bands were obtained at 2094 and 2048 cm^{-1}. The first one, already observed in the experiment without $C^{18}O$, is clearly resolved from the band at 2099 cm^{-1} (Figure 5, spectrum c). To explain the other band at 2048 cm^{-1} as the result of a simple shift of the band at 2050 cm^{-1} seems to be not justified considering that the band at 2050 cm^{-1} as the antisymmetric counterpart of the symmetric mode at 2114 cm^{-1} should be much weaker, similar to the antisymmetric modes of the other species at 2020 and 2004 cm^{-1}. The shift of 46 cm^{-1} from 2094 to 2048 cm^{-1} is what should be expected for a monocarbonyl with $C^{18}O$ instead of $C^{16}O$. The corresponding values for the fully exchanged dicarbonyl (Figure 5, spectrum a) are 45 and 46 cm^{-1} for the symmetric and antisymmetric stretchings, respectively.

From these experiments it can be concluded that a treatment of the dicarbonyl species in an atmosphere of diluted hydrogen at 200–250 °C results in a partial decarbonylation and in the formation of a monocarbonyl in the cavities of the zeolite. The dicarbonyl is stable, on the other hand, in flowing nitrogen up to 250 °C. The partial decarbonylation in the presence of diluted hydrogen at that temperature might be due, therefore, to a slow hydrogenation of the CO groups with the monocarbonyl as an intermediate. The fast complete decarbonylation at 250 °C in pure hydrogen and the observation that the intensity of the monocarbonyl band goes through a maximum during prolonged experiments with diluted hydrogen at 250 °C are in line with the above explanation.

The force constant of the CO stretching is higher in the monocarbonyl than in the starting dicarbonyl (the wavenumber of the CO stretching in the monocarbonyl is higher than the mean value of the two modes in $Rh^I(CO)_2^+$). Considering that only one CO ligand is competing for the π-electron density of Rh, one would expect the opposite result. A higher CO stretching frequency could be explained by an increase of the oxidation state of Rh, but such an oxidation can be probably ruled out in a reducing atmosphere. Also an interaction of the metal atom with a proton of an acid site in the neighborhood as proposed by Sachtler[21] to explain electron-deficient metal particles in acid zeolites seems hardly likely. As the result of the high Si:Al ratio (ca. 100) in the supports used, the acid sites are isolated and not available to the interaction with complexes localized on other acid sites.

Further, we could assume the formation of a dihydrogen complex on the surface, analogous to molecular dihydrogen complexes.[22] The formation of stable dihydrogen complexes requires, on the other hand, a critical amount of back-bonding, that was proposed to occur when the dinitrogen stretching frequency of the related complex with N_2 falls in the range $\nu(N_2) = 2060-2150$ cm^{-1}.[23] The dinitrogen stretching is in our case at significantly higher wavenumbers (see the next paragraph) and we should not expect, therefore, the formation of a stable dihydrogen complex on the surface. Indeed, we did not find any corresponding signals in the IR spectra, neither with H_2 nor with D_2. Even more significant to rule out a dihydrogen complex as the species formed during the treatment of the dicarbonyl with a hydrogen-containing gas flow is the observation that the same monocarbonyl is formed reversibly from the dinitrogen complexes also in the absence of any hydrogen (see the next paragraph).

As a remaining possibility, we should assume a change of the structure of the Rh complexes, i.e. a change of the number of framework oxygen atoms surrounding the Rh cation or a different arrangement of the oxygen ligands. In this connection, it might be interesting to refer to the three-coordinate molecular d^8 complexes of Rh, $RhX[P(C_6H_{11})_3]_2$, X = F, Cl, Br, and I, which are stabilized by the bulky phosphine ligands and which also form (for X = Cl, Br, and I) adducts with dinitrogen.[24] An example for a rearrangement of the oxygen ligand sphere has been found by extended X-ray absorption fine structure spectroscopy (EXAFS) upon partial decarbonylation of osmium

(21) Sachtler, W. M. H. *Acc. Chem. Res.* **1993**, *26*, 383–387 and references therein.
(22) Kubas, G. J. *Acc. Chem. Res.* **1988**, *21*, 120–128.
(23) (a) Morris, R. H.; Earl, K. A.; Luck, R. L.; Lazarowych, N. J.; Sella, A. *Inorg. Chem.* **1987**, *26*, 2674–2683. (b) Morris, R. H. *Inorg. Chem.* **1992**, *31*, 1471–1478.
(24) Van Gaal, H. L. M.; Van Den Bekerom, F. L. A. *Organomet. Chem.* **1977**, *134*, 237–248.

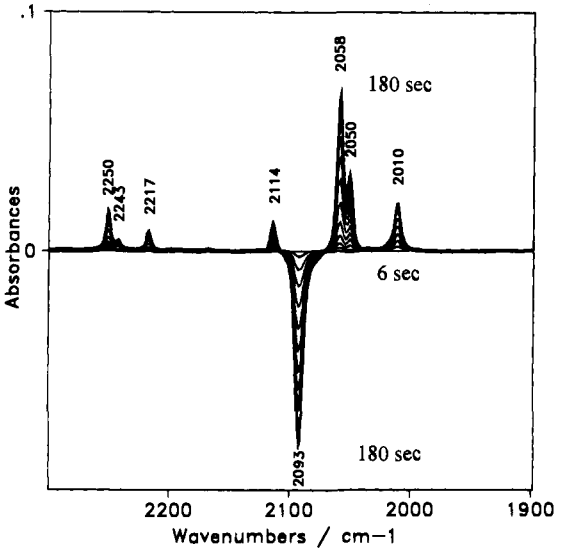

Figure 6. Infrared difference spectra in the carbonyl and dinitrogen stretching region of Rh/DAY obtained during the first 3 min after changing the gas flow from 10% H_2/N_2 to pure N_2 at 250 °C (time resolution of 6 s, not all spectra are shown for clarity). The spectrum at 250 °C before changing the gas composition from 10% H_2/N_2 to pure nitrogen is used as a reference.

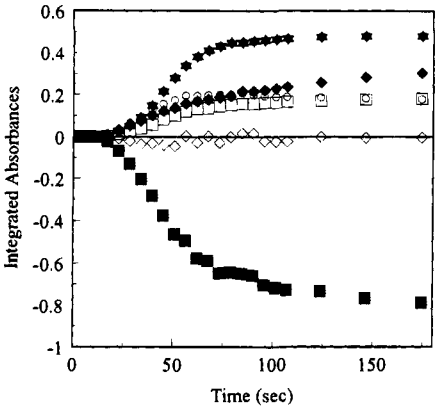

Figure 7. Evaluation of the integrated absorbances of the CO stretching bands as shown in Figure 5 during the formation of the dinitrogen complexes: ◆, 2114 + 2050 cm^{-1}; ■, 2093 cm^{-1}; ★, 2058 cm^{-1}; ○, 2010 cm^{-1}; ◇, sum of CO bands; □, sum of N_2 bands.

subcarbonyls on γ-alumina.[25] When osmium tricarbonyl on the surface was treated under vacuum at 300 °C, it lost one CO ligand and gained one surface oxygen ligand to maintain the coordinative saturation. It should be mentioned, however, that the resulting Os dicarbonyl has lower CO stretching frequencies than the starting tricarbonyl, whereas the change from the Rh dicarbonyl to a monocarbonyl in the present work is accompanied by an increase of the CO stretching frequency.

Formation of Surface Species with Molecular Nitrogen. Figure 6 shows the difference spectra obtained during the first 3 min after switching the gas flow from H_2/N_2 to pure N_2 at 250 °C. The intensity of the band of the monocarbonyl at 2093 cm^{-1} decreases, and simultaneously, new bands appear in the CO as well as in the N_2 stretching region. Figure 7 shows the evaluation of the integrated absorbances of the CO stretching bands during the formation of the nitrogen species. Assuming a similar extinction coefficient for all carbonyl species involved in the surface reaction, apparently no CO has been desorbed during the transformation of the monocarbonyl into several other

(25) Deutsch, S. E.; Chang, J.-R.; Gates, B. C. *Langmuir* **1993**, *9*, 1284–1289.

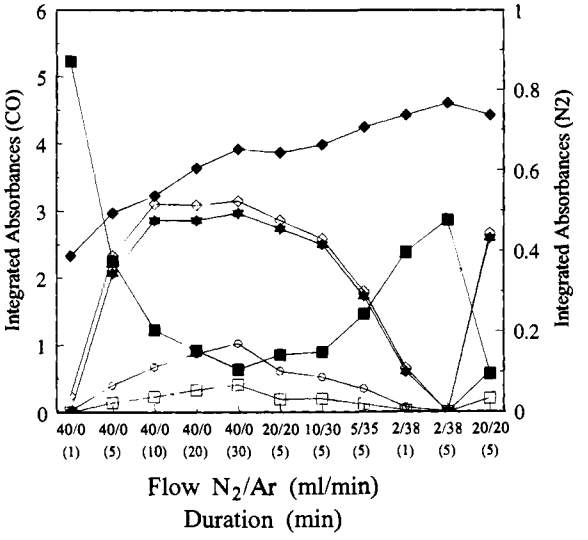

Figure 8. Evaluation of the integrated absorbances of the N_2 stretching bands (open symbols: ◇, 2251 cm^{-1}; ○, 2217 cm^{-1}; □, 2243 cm^{-1}, right ordinate) and of the CO stretching bands (full symbols: ◆, 2115 + 2051 cm^{-1}; ■, 2093 cm^{-1}; ★, 2060 cm^{-1}, left ordinate) of Rh/US-Ex in dependence on the time on the stream in pure N_2 and a subsequent substitution of nitrogen by argon at 200 °C.

carbonyl species. The bands at 2114 and 2050 cm^{-1} can be assigned to the already known Rh dicarbonyl, which is obviously formed back from the monocarbonyl. The other bands have to be assigned to new species.

The IR bands with wavenumbers higher than 2200 cm^{-1} are assigned to N_2 stretching vibrations. Its intensity is dependent on the flow conditions and the nitrogen partial pressure. Figure 8 shows the change of the intensity of the N_2 and CO stretching bands in dependence on the time on the stream at 200 °C and at substituting subsequently an increasing part of N_2 by argon. With decreasing partial pressure of N_2, the new surface species are converted again to the surface monocarbonyl. This conversion is reversible, as the subsequent formation of dinitrogen species at increasing N_2 pressure shows. Only the continuous increase in the intensity of the bands of the $Rh^I(CO)_2^+$ species seems to be irreversible.

Once formed, the dinitrogen species are stable in a flow of pure nitrogen also at lower temperatures. Figure 9 shows the spectra taken at 200 °C and after cooling the sample to room temperature. There is a small shift of all wavenumbers in dependence on the temperature, and we will use, if not referred to a particular experiment, the values obtained at room temperature to denote the IR bands. Besides this small band shift, there is only one significant difference between the two temperatures applied: the intensity of the monocarbonyl band at 2096 cm^{-1} increases at lower temperature, obviously at the expense of the band at 2014 cm^{-1}. The formation of the new species just described is, on the other hand, slow at temperatures lower than 200 °C, and the dicarbonyl species are rather formed at these conditions.

The results described in the previous paragraphs already provide a qualitative picture of the connections between the different bands in the spectra. A correlation analysis of the integrated absorbances in a series of related experiments shows on a more quantitative basis (Table 1) that the bands at 2252 and 2062 cm^{-1} behave in the same way and also those at 2244 and 2218 cm^{-1} are correlated, whereas the band at 2014 cm^{-1} seems to be not connected with any other new band. The spectra shown in Figures 6 and 9 indicate, on the other hand, that the

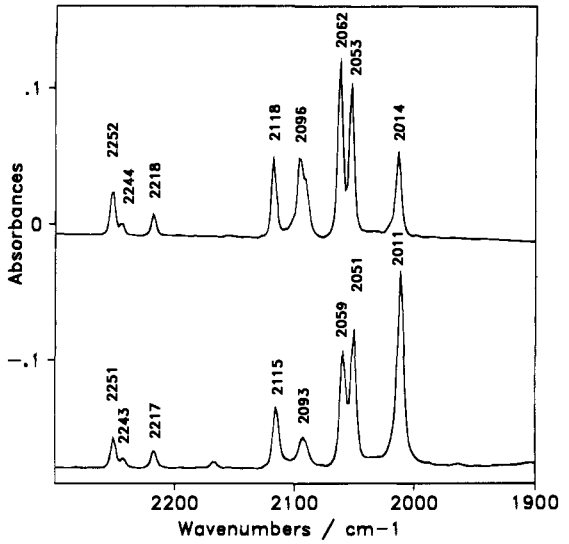

Figure 9. Infrared spectra in the carbonyl and dinitrogen stretching region after the formation of dinitrogen species on Rh/DAY in a flow of pure N_2 at 200 °C (lower spectrum) and after cooling in N_2 to 40 °C (upper spectrum).

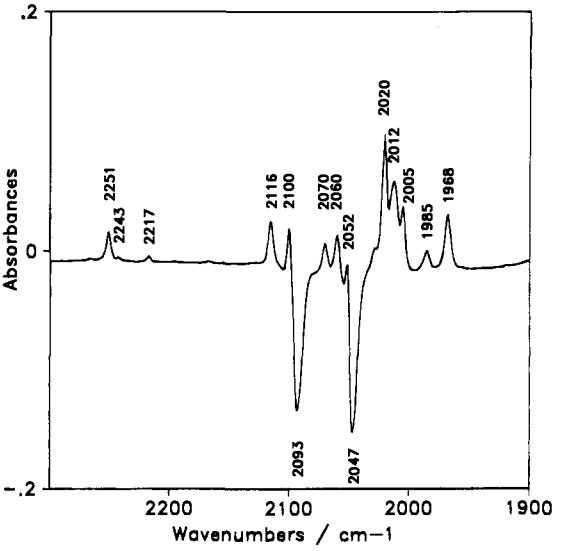

Figure 10. Infrared difference spectrum in the carbonyl and dinitrogen stretching region after interaction of pure N_2 at 250 °C with a Rh dicarbonyl on Rh/US-Ex containing both $C^{16}O$ and $C^{18}O$ as ligands.

two bands at 2096 and 2014 cm^{-1} are related in that the intensity of one band increases reversibly at the expense of the other one.

From these results, we conclude that a mixed surface complex containing both N_2 and CO as ligands, $Rh^I(CO)(N_2)^+$ (2252 and 2062 cm^{-1}), and a bis-dinitrogen complex, $Rh^I(N_2)_2^+$ (2244 and 2218 cm^{-1}), have been formed on the surface. Additionally, a second monocarbonyl, $Rh^I(CO)^+$ (2014 cm^{-1}), has been obtained on the surface. The nature of this second monocarbonyl remains open. The comparatively low wavenumber could be explained by the formation of a bridging CO species on Rh^+ sites as suggested by Rice et al.[15c] for bands in this frequency range. The Rh^+ cations are, on the other hand, fairly isolated from each other due to the high Si:Al ratio in the zeolite, and the formation of polynuclear Rh species seems hardly likely, especially in a nonreducing atmosphere.

To prove the assignment made in the previous paragraph, ligand exchange experiments using $^{15}N_2$ and $C^{18}O$ have been performed. For the formation of $C^{18}O$-containing species, it was necessary to start from the reactive monocarbonyl already exchanged with $C^{18}O$, as shown in Figure 5. The changes in the IR spectrum during the formation of the species containing dinitrogen are shown in Figure 10. As should be expected for the monocarbonyl, the carbonyl stretching bands at 2093 cm^{-1} ($C^{16}O$) and 2047 cm^{-1} ($C^{18}O$) decrease and, simultaneously, the bands of the new surface species appear. The bands in the N_2 stretching region are not affected by the introduction of $C^{18}O$. The bands at 2116 + 2052 cm^{-1}, 2100 + 2020 cm^{-1}, and 2070 + 2005 cm^{-1} belong to $Rh^I(CO)_2^+$, containing both $C^{16}O$ and $C^{18}O$ as already discussed. The band at 2060 cm^{-1}, which was assigned to $Rh^I(CO)(N_2)^+$, has the $C^{18}O$ counterpart, as should be expected, at 2012 cm^{-1} overlapping with the $C^{16}O$ stretching band at 2012 cm^{-1} of the second monocarbonyl, the $C^{18}O$ counterpart of which appears at 1968 cm^{-1}. The results are summarized in Table 2, together with the values calculated in the framework of an energy-separated force field.[26]

The changes, which take place in the nitrogen stretching region after the addition of $^{15}N_2$ to the stream of $^{14}N_2$ are shown in Figure 11. As should be expected, the bands of the pure $^{14}N_2$ components at 2251, 2243, and 2217 cm^{-1} decrease and new bands of the dinitrogen species containing $^{15}N_2$ appear in the spectrum. The wavenumbers obtained are again compared to those calculated on the basis of a force field calculation (Table 2). The agreement is satisfactory and verifies the assignment of the species. Additionally, we compared the intensities of the IR bands of the isotopically different $Rh^I(N_2)_2^+$ species with those calculated on the basis of the isotopic composition as obtained from the intensity ratio of the mono-N_2 species (bands at 2251 and 2177 cm^{-1}). The results are shown in Figure 12 for the available data. The good agreement between the calculated and observed intensities is an additional argument for the assignment.

For metal dicarbonyls with equivalent CO ligands, it has been shown that the ratio of the integrated absorbances of the antisymmetric (A_{as}) and symmetric (A_s) stretchings of CO is related to the bond angle (α) between the carbonyl groups as $A_{as}/A_s = \tan^2(\alpha/2)$.[26] For $Rh^I(CO)_2^+$ on dealuminated Y zeolites, we estimated a bond angle between the carbonyl groups at ca. 106°.[10] The same relation should be applicable also to dinitrogen complexes such as $Rh^I(N_2)_2^+$. The relationship between the integrated absorbances of the N_2 stretchings in the surface bis-dinitrogen complex at 2244 and at 2218 cm^{-1} is shown in Figure 13. Due to the low intensity of the dinitrogen

Table 1. Correlation Coefficients (Sample Size) of Integrated Absorbances of Dinitrogen and Carbonyl Stretching Bands Observed with Rh/US-Ex and Rh/DAY As Obtained by Multivariate Correlation Analysis (STATGRAPHICS)

wavenumber (cm^{-1})	2252	2244	2218	2118	2062	2053
2244	0.791 (93)					
2218	0.869 (93)	**0.968 (93)**				
2118	0.652 (93)	0.301 (93)	0.393 (93)			
2062	**0.987 (90)**	0.731 (90)	0.826 (90)	0.507 (95)		
2053	0.576 (93)	0.248 (93)	0.333 (93)	**0.994 (190)**	0.416 (95)	
2014	0.537 (62)	0.569 (62)	0.600 (62)	0.204 (70)	0.464 (65)	0.244 (70)

Table 2. Infrared Absorption Bands (cm^{-1}) of Well-Defined Surface Species with Different Isotopic Compositions at 200–250 °C

	N_2		CO		
species	obsd	calcd	obsd	calcd	$k(N_2)$ or k(CO) (N m^{-1})
$Rh^I(C^{16}O)(^{14}N_2)^+$	2251	*2252*	2060	*2061*	$k(N_2) = 2092$
$Rh^I(C^{18}O)(^{14}N_2)^+$			2012	*2011*	k(CO) = 1716
$Rh^I(C^{16}O)(^{15}N_2)^+$	2177	*2176*			
$Rh^I(^{14}N_2)_2^+$	2243 + 2217	*2243 + 2218*			
$Rh^I(^{15}N_2)_2^+$	2168 + 2144	*2167 + 2143*			$k(N_2) = 2053$
$Rh^I(^{14}N_2)(^{15}N_2)^+$	2232 + 2154	*2233 + 2153*			k(i) = 23
$Rh^I(C^{16}O)^+$			2093	*2095*	k(CO) = 1774
$Rh^I(C^{18}O)^+$			2047	*2045*	
$Rh^I(C^{16}O)^+$			2012	*2014*	k(CO) = 1639
$Rh^I(C^{18}O)^+$			1968	*1966*	
$Rh^I(C^{16}O)_2^+$			2114 + 2050	*2117 + 2052*	k(CO) = 1756
$Rh^I(C^{16}O)(C^{18}O)^+$			2099 + 2020	*2100 + 2019*	k(i) = 54
$Rh^I(C^{18}O)_2^+$			2069 + 2004	*2066 + 2003*	

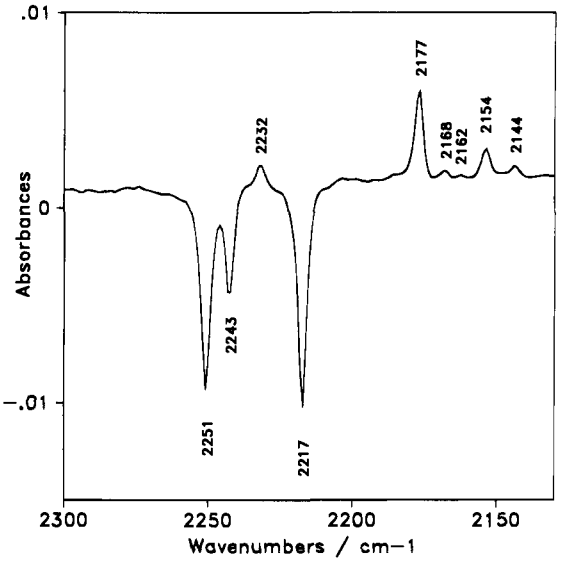

Figure 11. Infrared difference spectrum in the dinitrogen stretching region after the addition of $^{15}N_2$ to a flow of $^{14}N_2$ over dinitrogen species on Rh/DAY at 200 °C.

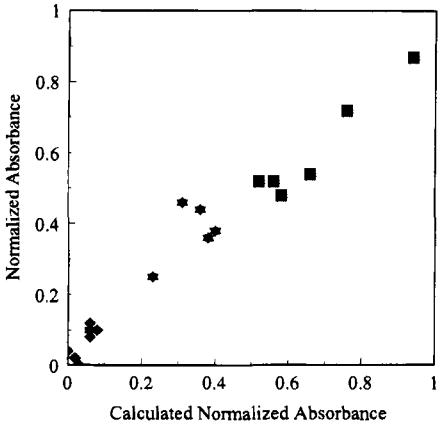

Figure 12. Normalized integrated absorbances of the bands of $Rh^I(^{14}N_2)_2^+$ (■), $Rh^I(^{15}N_2)_2^+$ (◆), and $Rh^I(^{14}N_2)(^{15}N_2)^+$ (★) as obtained in a series of experiments with different ratios $^{14}N_2/^{15}N_2$ in the gas flow compared with the values calculated from the absorbance ratios of the $^{14}N_2$ and $^{15}N_2$ bands of $Rh^I(CO)(N_2)^+$ in the same experiments.

stretching bands and the overlapping of the band at 2244 cm^{-1} with the dinitrogen stretching of the $Rh^I(CO)(N_2)^+$ complex at 2252 cm^{-1}, the data scatter more than those of the corresponding

(26) Braterman, P. S. *Metal Carbonyl Spectra*; Academic Press: London, 1975.

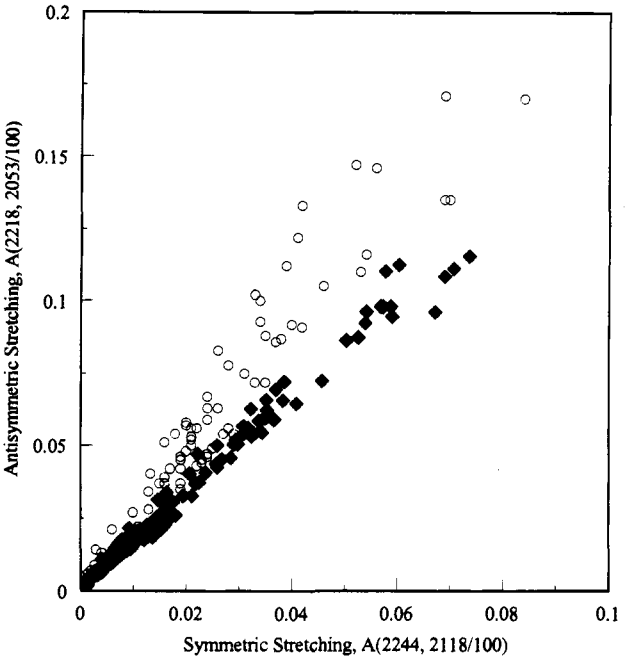

Figure 13. Correlation of the integrated absorbances of the symmetric (2244 cm^{-1}) and antisymmetric (2218 cm^{-1}) stretching bands of $Rh^I(N_2)_2^+$ (○) and of the corresponding bands of $Rh^I(CO)_2^+$ (2118 and 2053 cm^{-1}; divided by 100) (◆) on DAY and US-Ex at 40–250 °C.

carbonyl bands at 2118 and 2053 cm^{-1} (see also the correlation coefficients in Table 1). Nevertheless, the data allow the conclusion that the bond angle is larger (ca. 112°) between the nitrogen ligands in $Rh^I(N_2)_2^+$ than between the carbonyl ligands in $Rh^I(CO)_2^+$.

As already mentioned in the Introduction, Wang and Yates[8] and Wey et al.[9] found at low temperature or at high N_2 pressure, respectively, a chemisorption of N_2 on reduced Rh/Al_2O_3. The N_2 stretching band observed at 2256–2257 cm^{-1} has been assigned to dinitrogen adsorbed on metallic Rh sites, whereas bands at 2270–2276 cm^{-1} and at 2301–2303 cm^{-1} were attributed to different $Rh^{\delta+}$ sites in interaction with oxygen on partly oxidized samples. No indications for bis-dinitrogen surface complexes or mixed complexes containing N_2 and CO simultaneously have been observed.

Obviously, the species formed in the cavities of the zeolite are different from those found on the surface of a reduced Rh/Al_2O_3 sample. For a comparison, it should be considered that nitrogen interacts with quite different Rh samples. In case of Rh/Al_2O_3, N_2 reacts with a Rh surface which is reduced or partly oxidized by interaction with O_2 or CO. In the experiments

described in the present study, N_2 reacts with a subcarbonyl of Rh which is probably highly unsaturated due to the preceding partial decarbonylation. The zeolite framework contributes to the stabilization of the Rh complexes formed as already pointed out in the Introduction. This stabilization in a highly dealuminated zeolite and the reversible mutual conversion of the different surface species, one of which ($Rh^I(CO)_2^+$) is known to have Rh in the oxidation state +1, let us assume the same oxidation state also for the other surface species including those with dinitrogen.

The well-defined Rh dinitrogen complexes on the surface are rather to be compared with molecular dinitrogen complexes of Rh. In the Rh^I complex $[RhCl(N_2)((iPr)_3P)_2]$ (iPr = isopropyl), the dinitrogen ligand is bonded in an end-on coordination with an IR stretching vibration at 2100 cm^{-1}.[27] Together with the other ligands it forms a nearly planar coordination around the Rh. The same planar structure has been also proposed for the already mentioned dinitrogen adducts $RhX[P(C_6H_{11})_3]_2N_2$, X = Cl, Br, and I.[24] The N_2 stretchings are at 2100−2108 cm^{-1} in these complexes. Similarly as for $Rh^I(CO)_2^+$ (Figure 3), we would suggest also for the dinitrogen complexes a planar coordination with two zeolite framework oxygens as additional ligands to complete the coordination sphere. These oxygen atoms, instead of the electron-donating phosphine ligands as in the molecular complex described above, explain the significantly higher wavenumbers of the N_2 stretchings in the surface complexes. Related phosphine complexes with CO instead of N_2 as the ligand exhibit a CO stretching band at 1940−1950 cm^{-1},[24,27a] which is also significantly lower than the 2118 and 2053 cm^{-1} found for the dicarbonyl on the dealuminated Y zeolite.

In connection with the proposed localization of the well-defined surface species, it might be worth to mention that the results presented in the present paper were obtained with two different supports having the same faujasite structure and a similar chemical composition (Si:Al ≥ 100) but a different mesopore structure. US-Ex obtained by repeated hydrothermal treatment of the ammonium form of Y zeolite followed by an extraction of the nonframework alumina species with diluted hydrochloric acid has a high amount of mesopores in the region of 3−5 nm.[28] DAY obtained by a substitution of the framework aluminum by a controlled treatment with $SiCl_4$[29] is almost free of mesopores. The results are, nevertheless, very similar and we did not discriminate between them throughout the discussion. The essential property for the formation of the same well-defined surface compound is, obviously, the existence of isolated acid sites with identical crystallographic surroundings. By having a similar chemical composition and the same faujasite structure, this precondition is fulfilled for both supports.

By comparing the surface species with molecular analogues, it is interesting to focus on the force constants for CO and N_2 stretchings as shown in Table 2. The force constant of the N_2 stretching is higher in the mixed complex $Rh^I(CO)(N_2)^+$ than in the bis-dinitrogen complex $Rh^I(N_2)_2^+$, whereas just the opposite has been found for the CO stretching: in the dicarbonyl, k(CO) is higher than in $Rh^I(CO)(N_2)^+$. To the best of our knowledge, there are no molecular complexes of Rh with two dinitrogen ligands or mixed complexes with CO and N_2. But a similar relation has been found for related molecular complexes of Mo. The force constants in the mixed compound *trans*-$Mo(CO)(N_2)(dppe)_2$ (dppe = $Ph_2PCH_2CH_2PPh_2$) are k(CO) = 1307 N m^{-1} and $k(N_2)$ = 1810 N m^{-1}, whereas the corresponding values for the dicarbonyl and the bis-dinitrogen complexes are 1380 and 1658 N m^{-1}, respectively.[23a,30−32] These results are reasonably explained by the stronger π-acceptor ability of CO compared with the dinitrogen ligand.[1b,30,33]

Previously, we showed that the well-defined Rh dicarbonyl is an appropriate probe molecule to characterize the existence and the strengths of isolated acid sites in molecular sieves.[34] Due to the very sharp IR carbonyl bands of this surface compound, even small changes in the electron density of the Rh cations can be obtained by the shift of these bands. The electron density on Rh is, on the other hand, influenced by the electronic structure of the framework oxygens, which determine also the properties of the structural acid sites. As the N_2 molecule is a weaker base than CO, one would expect an even more sensitive response to changes of the electron density in the surrounding of Rh. Indeed, the N_2 ligand has been found in molecular complexes to be much more sensitive to effects of the trans ligand than the CO ligand.[23a] Thus, the dinitrogen complexes might be used as a sensitive probe molecule to characterize different acid sites in molecular sieves.

Conclusion

The well-defined Rh dicarbonyl species $Rh^I(CO)_2^+$ supported on dealuminated Y zeolite has been found to be a useful starting material to synthesize new surface complexes of Rh. Time-resolved IR spectroscopy has been used to monitor the reactions on the surface. The following results have been obtained:

(1) A partial decarbonylation of the surface dicarbonyl in a flow of diluted hydrogen at 200−250 °C results in the formation of a reactive monocarbonyl with an IR carbonyl stretching band at 2096 cm^{-1}. This monocarbonyl reacts with pure nitrogen to form surface complexes of Rh containing dinitrogen as ligands. These complexes are stable in flowing pure nitrogen at temperatures up to 250 °C. They react with CO, yielding the dicarbonyl, and with H_2/N_2, forming reversibly the intermediate monocarbonyl. Additionally, a different monocarbonyl has been obtained on the surface with ν(CO) = 2014 cm^{-1}.

(2) An evaluation of the integrated band absorbances of the CO and N_2 stretching bands and ligand exchange experiments with D_2, $C^{18}O$, and $^{15}N_2$ combined with the corresponding force field calculations reveals that two well-defined dinitrogen complexes have been formed on the surface: $Rh^I(N_2)_2^+$ with $\nu(N_2)$ = 2244 and 2218 cm^{-1} and a mixed carbonyl−dinitrogen complex $Rh^I(CO)(N_2)^+$ with $\nu(N_2)$ = 2252 and ν(CO) = 2062 cm^{-1}.

(3) Using the integrated absorbances of the symmetric and antisymmetric N_2 stretchings in $Rh^I(N_2)_2^+$, a bond angle between the two dinitrogen ligands of ca. 112° has been estimated, which is slightly larger than that estimated at 106° between the carbonyl ligands in $Rh^I(CO)_2^+$.

(4) The formation of the same nitrogen-containing complexes has been found on two differently dealuminated Y zeolites with (US-Ex) and without (DAY) mesopores. This agreement supports the localization of the well-defined species on isolated

(27) (a) Busetto, C.; D'Alfonso, A.; Maspero, F.; Perego, G.; Zazzetta, A. *J. Chem. Soc., Dalton Trans.* **1977**, 1828−1834. (b) Thorn, D. L.; Tulip, T. H.; Ibers, J. A. *J. Chem. Soc., Dalton Trans.* **1979**, 2022−2025.

(28) Stach, H.; Lohse, U.; Thamm, H.; Schirmer, W. *Zeolites* **1986**, *6*, 74−90.

(29) Beyer, H. K.; Belenykaya, I. In *Catalysis by Zeolites*; Imelik, B., et al., Eds.; Elsevier: Amsterdam, 1980; pp 203−210.

(30) Sato, M.; Tatsumi, T.; Kodama, T.; Hidai, M.; Uchida, T.; Uchida, Y. *J. Am. Chem. Soc.* **1978**, *100*, 4447−4452.

(31) George, T. A.; Seibold, C. D. *Inorg. Chem.* **1973**, *12*, 2548−2552.

(32) (a) Hidai, M.; Tominari, K.; Uchida, Y. *J. Am. Chem. Soc.* **1972**, *94*, 110−114. (b) Darensbourg, D. J. *Inorg. Chem.* **1972**, *11*, 1436−1437.

(33) Darensbourg, D. J. *Inorg. Chem.* **1971**, *10*, 2399−2403.

(34) Burkhardt, I.; Jahn, E.; Miessner, H. *J. Phys. Chem.* **1992**, *96*, 2259−2265.

structural acid sites at the remaining Al atoms in the zeolite framework.

(5) A comparison of the force constants of N_2 and CO stretchings in the bis-dinitrogen and the dicarbonyl complexes with those in the mixed $Rh^I(CO)(N_2)^+$ complex shows the effect of the weaker π-acceptor ability of the N_2 ligand compared with the carbonyl ligand.

(6) The absence of related molecular complexes of Rh with two dinitrogen ligands or of mixed complexes with a carbonyl and a dinitrogen ligand together shows the ability of zeolites with a high Si:Al ratio and, consequently, with isolated acid sites to stabilize unexpected well-defined surface complexes of transition metals.

Acknowledgment. Financial support by the Deutsche Wissenschaftliche Gesellschaft für Erdöl, Erdgas und Kohle e.V., DGMK-Projekt 470/AIF Forschungsvorhaben 268 D, and by a grant from the Fonds der Chemischen Industrie is gratefully acknowledged. The author thanks DEGUSSA (Germany) for providing the DAY and Dr. U. Lohse for providing the US-Ex zeolite. The author thanks Mrs. P. Haase and Mrs. P. Rössler for experimental assistance.